

# THE PERFORMANCE OF KARAFILLIS-BOYCE YIELD FUNCTION ON DETERMINATION OF FORMING LIMIT DIAGRAMS

*M. Ganjani and A. Assempour\**

*Department of Mechanical Engineering, Sharif University of Technology  
Azadi Avenue P.O. Box 11365-9567, Tehran, Iran  
assem@sharif.edu*

\*Corresponding Author

(Received: June 25, 2006 - Accepted in Revised Form: January 18, 2007)

**Abstract** Forming Limit Diagrams are useful tools for evaluation of formability in the sheet metals. In this paper the effects of yield criteria on predictions of the right and left-hand sides of forming limit diagrams (FLDs) are investigated. In prediction of FLD, Hosford 1979, "Karafillis-Boyce" (K-B) and BBC2000 anisotropy yield functions have been applied. Whereas the prediction of FLD is based on the "Marciniak and Kuczynski" model, thus a numerical approach using the Newton-Raphson method has been used. Forming Limit Diagrams have been obtained for Al 6111-T4 and AA5XXX alloys and results have been compared with published experimental data. Results indicate that predictions of FLD are very sensitive to selection of yield criterion. Also it was found that the FLD of K - B yield function has a better agreement than that by other yield criteria.

**Keywords** Marciniak and Kuczynski Model, Karafillis and Boyce, Hosford 1979, BBC2000, Yield Function, Newton-Raphson Method

**چکیده** منحنی‌های حد شکل‌دهی ابزارهای مفید برای تخمین شکل‌پذیری ورق‌های فلزی می‌باشند. در این مقاله تاثیر معیارهای تسلیم مختلف روی محاسبه سمت راست و چپ منحنی‌های حد شکل‌دهی بررسی می‌شود. در محاسبه منحنی‌های حد شکل‌دهی، معیارهای تسلیم ناهمسانگردی چون هاسفورد ۱۹۷۹، کارافیلیس - بویس و بی‌بی‌سی ۲۰۰۰ اعمال شده است. از آنجا که بدست آوردن منحنی‌های حد شکل‌دهی بر پایه مدل مارشینیاک - کوزینسکی می‌باشد، بنابراین روش عددی نیوتن - رافسون استفاده شده است. منحنی‌های حد شکل‌دهی برای آلیاژهای AA5XXX و Al 6111-T4 استخراج گشته و نتایج آن با داده‌های تجربی منتشر شده در بقیه مقالات مقایسه شده است. این نتایج نشان می‌دهد که منحنی‌های حد شکل‌دهی به انتخاب نوع تابع تسلیم حساس هستند. همچنین مشاهده شده که منحنی حد شکل‌دهی منتهی از تابع تسلیم کارافیلیس - بویس تطابق بهتری با نتایج تجربی نسبت به بقیه توابع تسلیم دارد.

## 1. INTRODUCTION

In sheet metal operation, the amount of deformation is restricted by the occurrence of localized necking. Experimental investigations revealed that localized necking of sheet metals could be well described by a diagram in principal strain plane, namely Forming limit diagram (FLD). Thus the FLD is convenient tool to be used as the reference in evaluation of the formability in sheet metals.

Keeler and Backofen [1] and Goodwin [2]

introduced the concept of the forming limit diagram (FLD). Keeler [3] found the material properties have great effect on the strain distribution in biaxial stretching of sheet metals. Most theoretical and numerical studies on FLD analysis have been established on the so-called M-K approach developed by Marciniak and Kuczynski [4]. Marciniak et al. [5] slightly modified their original model to study the effects of plastic anisotropy. Their analytical results agree with experimental evidence for steel and copper, but were not accurate for aluminum.

Van Minh, et al. [6], Yamaguchi and Mellor [7], Tadros and Mellor [8] examined the effects of different types of initial non-uniformity on FLD. Barata da Rocha et al. [9] used the M–K method to predict FLD. They also used Hill’s 1948 yield criterion and analyzed the influence of the directional r-values. Kuroda and Tvergaard [10] investigated the influence of different orthotropic yield criteria in the M–K model and showed that disorientations of the orthotropic axes inside and outside the necking band can lead to significant differences in FLD prediction. Cao et al. [11] predicted localized thinning of sheet metal alloys for linear and nonlinear strain paths in the Marciniak-Kuczynski (M-K) model. Kuroda and Tvergaard [12] studied the influence of the yield criterion on Forming Limit Diagram by using the M-K model. Butuc et al. [13] used the M–K model and proposed a solution scheme based on a Newton–Raphson solver in order to determine the unknown parameters in the M–K model. Banabic et al. [14] compared different modeling approaches to predict the forming limit diagram (a finite element based approach, the M–K model, the Hora et al., Swift’s diffuse and Hill’s localized necking approach) using an orthotropic yield criterion BBC2003. They showed that the results of the M–K model and the finite element based approach are very close to each other and agreed very well with the experimental necking FLD.

A thorough review of the effects of yield surface shape on the prediction of FLDs was offered by Barlat [22]. In his work, several important characteristics of the yield surface are identified and a parameter is introduced that quantifies some of the differences between various yield criteria. This parameter,  $P$ , defined as the ratio of the yield stress in plane strain to that in balanced-biaxial tension has been shown to correlate well with predictions of limit strains based on the M-K analysis.

The purpose of this paper is to investigate the effect of three yield surface shape namely Hosford 1979, “Karafillis - Boyce” (K-B) and BBC2000 on prediction of the right and left hand sides of Forming Limit Diagrams. Thus a developed numerical method on M-K model for prediction of the FLD is applied. The numerical approach is based on the Newton-Raphson method. For calculating FLD, two hardening laws such as

Power law and Voce hardening laws [15] are employed. Also, the predicted FLD is compared with the experimental data for Al 6111-T4 and AA5XXX metals.

## 2. YIELD CRITERIA

While there exists numerous yield criteria that incorporate the effects of plastic anisotropy, we examine the effects of three specific criteria in order to find a general rule for making judgment on the effects of plastic anisotropy on forming limit. The first of these is Hosford 1979’s yield criterion:

$$\sigma_1^a + \sigma_2^a + R(\sigma_1 - \sigma_2)^a = (R+1) \bar{\sigma}_y^a \quad (1)$$

where  $\sigma_1$  and  $\sigma_2$  are the in-plane principal stresses and  $\bar{\sigma}_y$  is the equivalent stress, in this case, equal to the yield stress in uniaxial tension. The coefficient  $R$  is normal anisotropy and is defined by:

$$R = \frac{1}{4}(R_0 + 2R_{45} + R_{90}) \quad (2)$$

where  $R_0$ ,  $R_{45}$  and  $R_{90}$  are the ratios of transverse to through-thickness strains under uniaxial tension at 0, 45° and 90° to the rolling direction. This criterion is based on upper-bound crystallographic calculations. The suggested exponent,  $a$ , is 6 for BCC materials and 8 for FCC materials. This criterion has been plotted for both cases for various values of  $R$  in Figures 1 and 2, respectively. As shown in the figures, the yield surfaces are quite flat and the positions of plane strain relative to that of balanced-biaxial stretching are quite insensitive to the value of  $R$ .

The second yield surface of the anisotropic material with orthotropic symmetry is described by a non-quadratic yield criterion developed by “Karafillis and Boyce” [15]. The K-B yield criterion was constructed by mixing two yield functions,  $\Psi_1$  and  $\Psi_2$ . As shown in Equations 3-5,  $\Psi_1$  represents a yield locus located between the Tresca yield locus and the von Mises yield locus and  $\Psi_2$  varies by the von Mises to a theoretical

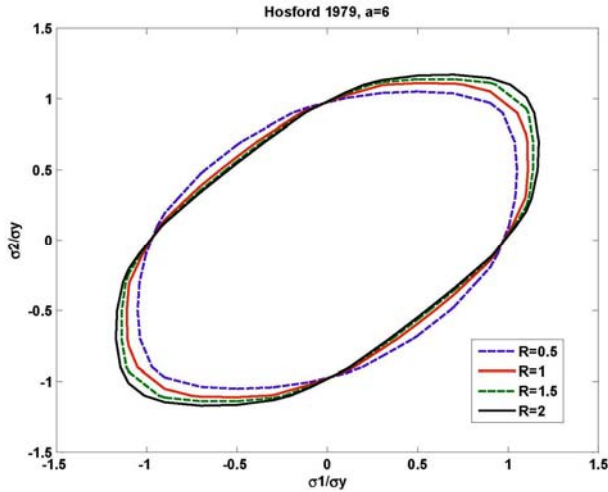


**Figure 1.** Hosford's yield criterion with an exponent of 6 for various values of  $R$ .

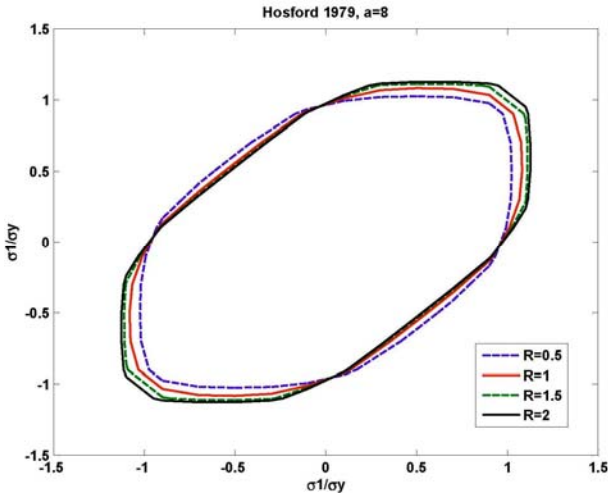


**Figure 2.** Hosford's yield criterion with an exponent of 8 for various values of  $R$ .

upper bound as  $a$  changes from 2 to  $\infty$ .

$$\bar{\sigma}_y = \left[ \frac{(1-C)\Psi_1 + C\Psi_2}{2} \right]^{\frac{1}{a}} \quad (3)$$

where,

$$\Psi_1 = |S_2 - S_3|^a + |S_1 - S_3|^a + |S_1 - S_2|^a \quad (4)$$

$$\Psi_2 = \frac{3^a}{2^{a-1} + 1} (|S_1|^a + |S_2|^a + |S_3|^a) \quad (5)$$

$a$  and  $c$  are material constants and  $S_i$  is the principal values of the isotropic plasticity equivalent stress tensor and  $\bar{\sigma}_y$  is the average yield stress in uniaxial tension obtained experimentally. A fourth order tensorial operator,  $L$ , introduces the material anisotropy, i.e.

$$S = L : \sigma \quad (6)$$

Where  $s$  is isotropic plasticity stress tensor,  $\sigma$  is the Cauchy stress in the anisotropic material:

$$\sigma = [\sigma_{11} \ \sigma_{22} \ \sigma_{33} \ \sigma_{31} \ \sigma_{23} \ \sigma_{12}] \quad (7)$$

and  $L$  is a fully symmetric and traceless fourth order tensor:

$$L = \begin{bmatrix} (C_2 + C_3)/3 & -C_3/3 & -C_2/3 & 0 & 0 & 0 \\ -C_3/3 & (C_3 + C_1)/3 & -C_1/3 & 0 & 0 & 0 \\ -C_2/3 & -C_1/3 & (C_1 + C_2)/3 & 0 & 0 & 0 \\ 0 & 0 & 0 & C_4 & 0 & 0 \\ 0 & 0 & 0 & 0 & C_5 & 0 \\ 0 & 0 & 0 & 0 & 0 & C_6 \end{bmatrix} \quad (8)$$

Where  $c_1, c_2, \dots, c_6$  are material constants. The last criterion is BBC2000 yield criterion. This yield function is a new yield criterion for orthotropic sheet metals under plane stress conditions. It is derived for the one proposed by Barlat and Lian in 1989 [22]. Two additional coefficients, namely  $\bar{b}$  and  $\bar{c}$ , have been introduced in order to allow a better representation of the orthotropic sheet metals plastic behavior. The equivalent stress is defined by the following relationship:

$$\bar{\sigma} = \left[ \frac{\bar{a}(\bar{b}\Gamma + \bar{c}\Psi)^{2K} + \bar{a}(\bar{b}\Gamma - \bar{c}\Psi)^{2K} + (1-\bar{a})(2\bar{c}\Psi)^{2K}}{2K} \right]^{\frac{1}{2K}} \quad (9)$$

Where  $\bar{a}, \bar{b}, \bar{c}$  and  $K$  are material parameters, while  $\Gamma$  and  $\Psi$  are the functions of the second and third invariants of a fictitious deviatoric stress tensor  $S = L : \sigma$ , where  $L$  is a fourth order tensor

described in Equation 8. Hence, in the reference system associated to the directions of plastic orthotropy, the tensor  $L$  has six non-zero components for 3D conditions and four components for a plane stress state. Let  $(x, y, z)$  be the reference frame associated to the directions of plastic orthotropy. For a rolled sheet,  $x$ ,  $y$ , and  $z$  represent the rolling direction, the transverse direction, and the perpendicular to the plane of the sheet metal, respectively. The components of the  $s$  tensor can be expressed as follows in this frame:

$$\begin{aligned} S_{11} &= d\sigma_{11} + e\sigma_{11}, & S_{22} &= e\sigma_{22} + f\sigma_{22}, \\ S_{33} &= -(d+e)\sigma_{11}, & & -(e+f)\sigma_{22}, \\ S_{12} &= g\sigma_{12}, & S_{21} &= g\sigma_{21}, \\ S_{23} &= S_{32} = 0, & S_{31} &= S_{13} = 0 \end{aligned} \quad (10)$$

Where  $d$ ,  $e$ ,  $f$  and  $g$ , the four independent components of the tensor  $L$ , are anisotropy coefficients of material. The second and third invariants of the deviatoric tensor  $s$  have the following expressions:

$$J_2 = S_{kk}^2 - \det S_{ij}, \quad J_3 = -(\det S_{ij})S_{kk} \quad (11)$$

where the Greek indices take the values 1 and 2.

$$I_2 = S_{kk}, \quad I_3 = \det S_{ij} \quad (12)$$

The quantities are not affected by the rotations that leave unchanged the third axis (ND). Thus, in the case of the plane stress of sheet metals, we can use  $I_2$  and  $I_3$  instead of  $J_2$  and  $J_3$  in order to define the functions  $\Gamma$  and  $\Psi$ . We have adopted the following expressions for these functions:

$$\begin{aligned} \Gamma &= I_2, \\ \Psi &= \left[ \left( \frac{I_2}{2} \right)^2 - I_3 \right]^{\frac{1}{2}} \end{aligned} \quad (13)$$

By using Equations 11-13, we can express  $\Gamma$  and  $\Psi$  as explicit dependences of the actual stress components;

$$\begin{aligned} \Gamma &= M\sigma_{11} + N\sigma_{22}, \\ \Psi &= \sqrt{(P\sigma_{11} + Q\sigma_{22})^2 + R\sigma_{12}\sigma_{21}} \end{aligned} \quad (14)$$

where,

$$M = d + e, \quad N = e + f \quad (15)$$

and

$$P = \frac{d - e}{2}, \quad Q = \frac{e - f}{2}, \quad R = g^2 \quad (16)$$

The  $K$  value is set in accordance with the crystallographic structure of the material:  $K = 3$  for BCC alloys, and  $K = 3$  for FCC alloys.

These criteria have been plotted for AA5XXX in Figure 3. Material constants of this metal for these yield criteria are listed in Tables 1 and 3.

As shown in Figure 3, at the position balanced -biaxial stretching, the Hosford's yield surface is coincided to the BBC2000's yield surface. At other positions, the differences between these two yield function is negligible. But the differences between Karafillis - Boyce yield surface and other two yield surfaces are sensible.

### 3. REVIEW OF MARCINIAK AND KUCZYNSKI MODEL

In this paper, to obtain the limit strains, the "Marciniak and Kuczynski" (M-K) model [4] has been used. In this model, it has been assumed that there is a narrow groove in the sheet surface. Thus the sheet is composed of safe area and a groove area which are denoted by 'a' and 'b', respectively. Figure 4 shows these areas. This groove leads to localized necking in the sheet. For modeling the groove, an imperfection factor is introduced which represents the thickness ratio  $f = t_b / t_a$ , where "t" denotes the thickness. Stress components are imposed at rolling and transverse directions in the safe area and cause the progress of strain increments in both the safe and the groove areas. Necking occurs when the effective strain in the groove area is 10 times of that in the safe area.

During the entire process, the force equilibrium equations at groove direction must be satisfied as

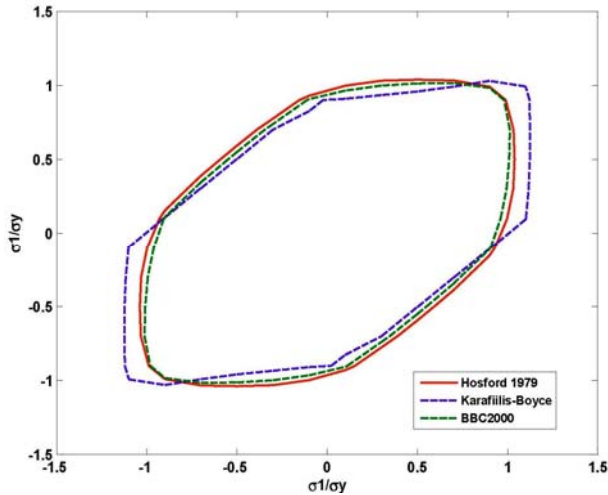


Figure 3. Comparison of different yield surfaces.

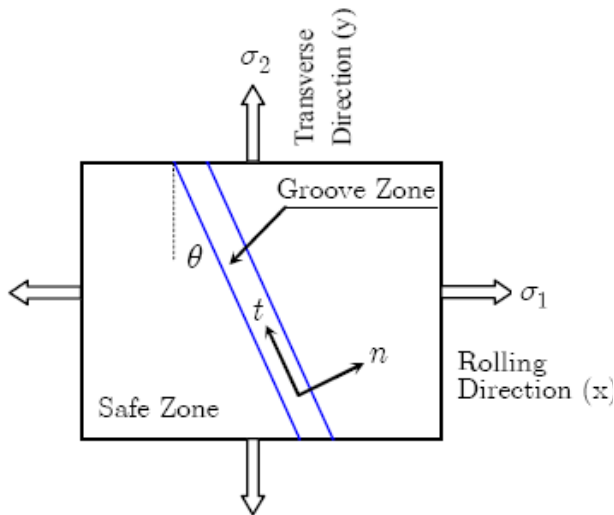


Figure 4. Assumption of a narrow groove in the sheet surface for prediction of FLD in the M - K model.

follows:

$$\begin{aligned} F_{nt}^a &= F_{nt}^b \\ F_{nn}^a &= F_{nn}^b \end{aligned} \quad (17)$$

where  $F_{nn}$  and  $F_{nt}$  are forces in the normal and tangential directions in the groove. By introducing the stress state in these areas, Equation 17 could be

rewritten as follows:

$$\sigma_{nt}^a \exp(\varepsilon_3^a) t_0^a = \sigma_{nt}^b \exp(\varepsilon_3^b) t_0^b \quad (18)$$

$$\sigma_{nn}^a \exp(\varepsilon_3^a) t_0^a = \sigma_{nn}^b \exp(\varepsilon_3^b) t_0^b$$

where  $\sigma_{nn}$  and  $\sigma_{nt}$  are stress components in the “n” and “t” directions,  $t_0^a$  and  $t_0^b$  are initial thicknesses in the safe and groove regions, respectively. Non-uniformity factor,  $f$ , can be expressed as a function of the initial defect:

$$f = f_0 \exp(\varepsilon_3^b - \varepsilon_3^a) \quad (19)$$

Herein  $f_0$  is the initial non-uniformity factor and denotes by  $t_0^b/t_0^a$ , and  $\varepsilon_3$  is the strain in thickness direction calculated by incompressibility condition:

$$\varepsilon_3 = -(\varepsilon_1 + \varepsilon_2) \quad (20)$$

Thus, force equilibrium conditions are summarized as:

$$\begin{aligned} f \sigma_{nn}^b &= \sigma_{nn}^b \\ f \sigma_{nt}^b &= \sigma_{nt}^a \end{aligned} \quad (21)$$

It is assumed that the strain increments parallel to the groove are the same in both regions (compatibility condition):

$$d\varepsilon_{tt}^b = d\varepsilon_{tt}^a \quad (22)$$

By using the force equilibrium and compatibility conditions, the unknown parameters are obtained. The unknown parameters are including stress and strain components, whereas, using flow rule, the strain components are related to effective strain and stress state:

$$d\varepsilon_{ij} = d\bar{\varepsilon} \frac{\partial \bar{\sigma}}{\partial \sigma_{ij}} \quad (23)$$

Thus the unknown parameters are reduced to stress components and effective strain.

**TABLE 1. Material Constants Describing the K - B Yield Function [18].**

Metal	a	c	c <sub>1</sub>	c <sub>2</sub>	c <sub>3</sub>	c <sub>6</sub>
Al 6111-T4	26	0.63	1.03	1.08	0.96	0.48
AA5XXX	26	0.63	1.05	0.80	1.07	0.99

**TABLE 2. Material Constants Describing the Hardening Laws.**

Power law [19]			
Metal	K	ε <sub>0</sub>	n
Al 6111-T4	489.37	0.0127	0.233
Voce hardening law [20]			
Metal	A	B	C
AA5XXX	416.067	273.068	8.301

**TABLE 3. Mechanical Constants Describing BBC2000 and Hosford Yield Functions for AA5XXX.**

$\bar{a}$	$\bar{b}$	$\bar{c}$	M	N	P	Q	K	R
0.663	0.982	0.730	0.507	0.504	0.726	-0.725	4	0.63

#### 4. COMPUTATION PROCESS

To calculate the limit strains, the safe region is loaded, i.e. it is assumed the safe region is stretched with constant stress relation  $\alpha$ . For this purpose, a value for  $\alpha$ , between 0 and 1 is selected and note that this value must remain constant at entire time during the process. At starting, a small value for effective strain increment  $d\bar{\epsilon}_a$  (for example 0.0001) is assumed. Substituting  $\bar{\epsilon}_a$  in the hardening law, the effective stress  $\bar{\sigma}_Y$  is obtained. Since the effective stresses by hardening law and yield function are equal, thus  $\sigma_x^a$  and  $\sigma_y^a$  can be obtained. A relationship between effective strain

and effective stress can be represented by the so-called Power law:

$$\bar{\sigma}_Y = K(\epsilon_0 + \bar{\epsilon})^n \quad (24)$$

where,  $K$  is the strength coefficient,  $\epsilon_0$  is the pre-strain and  $n$  is the hardening law exponent. Also Voce [15] hardening law has been used to describe behavior of aluminum alloys that are insensitive to the strain-rate sensitively:

$$\bar{\sigma}_Y = A - B \exp(-C\bar{\epsilon}) \quad (25)$$

Where  $A$ ,  $B$  and  $C$  are material constants. Using the assumed  $d\bar{\epsilon}_a$ , stress components and flow rule,

strain components  $d\epsilon_x^a$  and  $d\epsilon_y^a$  are calculated.

Since the groove has an angle with respect to transverse direction, it is required to find stress and strain states in the groove direction. This work is needed for satisfying the compatibility and force equilibrium conditions. Using the rotation matrix, the vectors for strain and stress tensors are changed to the groove system of coordinates:

$$\sigma^{ntz} = T \sigma^{xyz} T^T = \begin{bmatrix} \sigma_{nn} & \sigma_{nt} \\ \sigma_{nt} & \sigma_{tt} \end{bmatrix} \quad (26)$$

with,

$$T = \begin{bmatrix} \cos(\theta) & \sin(\theta) \\ -\sin(\theta) & \cos(\theta) \end{bmatrix} \quad (27)$$

where  $T$  is the rotation matrix and  $T^T$  is transpose of rotation matrix. In this paper, for calculating the unknown parameters at groove region, the Newton-Raphson method is applied. Consider  $N$  functional  $F_i$  relations to be zeroed involving variables  $x_i$ ,  $i=1,2,\dots,N$ . as follows:

$$F_i(x_1, x_2, \dots, x_N) = 0 \quad i=1,2,\dots,N. \quad (28)$$

Using Taylor series, functions  $F_i$  can be expanded as follows:

$$F_i(x + \delta x) = F_i(x) + \sum_{j=1}^N \frac{\partial F_i}{\partial x_j} \delta x_j + O(\delta x^2) \quad (29)$$

In matrix notation, Equation 29 is reduced to:

$$F(x+\delta x) = F(x) + J \cdot \delta x + O(\delta x^2) \quad (30)$$

Where  $J$  is the matrix of partial derivatives and is called the Jacobian matrix.

$$J_{ij} = \frac{\partial F_i}{\partial x_j} \quad (31)$$

By neglecting terms of order  $\delta x^2$  and higher and by setting  $F(x+\delta x)=0$ , we obtain a set of nonlinear equations:

$$J \cdot \delta x + F = 0 \quad (32)$$

or,

$$\delta x = -J^{-1} \cdot F \quad (33)$$

Then, the variable  $\delta x$  is added to the solution vector:

$$x_{\text{new}} = x_{\text{old}} + \lambda \delta x \quad (34)$$

where  $\lambda$  is the Newton step length. Using a backtracking algorithm, an acceptable  $\lambda$  can be found. The following steps must be considered as the simplest backtracking line search to find  $\lambda$ :

**Step 1.** Set  $\lambda = 1$ .

**Step 2.** While:

$$g(x_{\text{new}}) > g(x_{\text{old}}) + \frac{\nabla g(x) \cdot (x_{\text{new}} - x_{\text{old}})}{10^4} \quad (35)$$

set  $\lambda = \lambda s$ .

**Step 3.** Set  $\lambda_k = \lambda$ .

Equation 35 is suggested by Armijo [19] as the condition for finding the optimum  $\lambda$ . In this equation  $g(x)$  is defined as;

$$g(x) = F \cdot F \quad (36)$$

Typically,  $s = 0.8$  or  $0.5$ , meaning that based on the

linear extrapolation, a small decrease in  $g(x)$  is accepted. To exit the Newton's calculation loops, it is required to define a criterion. In the present formulations, there exists a vector of function which has four components. All components of this vector have the same important rank. Thus, the maximum value among these components has been selected to be compared with the tolerance in the Newton's loop. i.e.:

$$\|F\|_{\infty} = \max_{i=1}^4 |F_i| \quad (37)$$

This is called  $\infty$  - norm. Since the unknown parameters in this region are including,  $\sigma_{nn}^b$ ,  $\sigma_{tt}^b$ ,  $\sigma_{nt}^b$  and  $d\bar{\epsilon}_b$ , the vector of values  $x$  is defined as:

$$x = \left[ \sigma_{nn}^b \quad \sigma_{tt}^b \quad \sigma_{nt}^b \quad d\bar{\epsilon}_b \right]^T \quad (38)$$

Using the compatibility and force equilibrium conditions, three equations for the vector of functions are obtaining. In this paper, the energy relation is used as the 4th equation:

$$d\epsilon_{nn}^b \sigma_{nn}^b + d\epsilon_{tt}^b \sigma_{tt}^b + d\epsilon_{nt}^b \sigma_{nt}^b = d\bar{\epsilon}_b \bar{\sigma}_Y \quad (39)$$

Thus, vector of functions,  $F$  is introduced as follows:

$$F = \left[ F_1 \quad F_2 \quad F_3 \quad F_4 \right]^T \quad (40)$$

where,

$$F_1 = \frac{d\epsilon_{nn}^b \sigma_{nn}^b + d\epsilon_{tt}^b \sigma_{tt}^b + d\epsilon_{nt}^b \sigma_{nt}^b}{d\bar{\epsilon}_b \bar{\sigma}_Y} - 1 = 0 \quad (41)$$

$$F_2 = \frac{d\epsilon_{tt}^b}{d\epsilon_{tt}^a} - 1 = 0 \quad (42)$$

$$F_3 = f \frac{\sigma_{nn}^b}{\sigma_{nn}^a} - 1 = 0 \quad (43)$$

$$F_4 = f \frac{\sigma_{nt}^b}{\sigma_{nt}^b} - 1 = 0 \quad (44)$$

and the Jacobian matrix is written as:

$$J = \begin{bmatrix} \frac{\partial F_1}{\partial \sigma_{nn}^b} & \frac{\partial F_1}{\partial \sigma_{tt}^b} & \frac{\partial F_1}{\partial \sigma_{nt}^b} & \frac{\partial F_1}{d\bar{\epsilon}_b} \\ \frac{\partial F_2}{\partial \sigma_{nn}^b} & \frac{\partial F_2}{\partial \sigma_{tt}^b} & \frac{\partial F_2}{\partial \sigma_{nt}^b} & \frac{\partial F_2}{d\bar{\epsilon}_b} \\ \frac{\partial F_3}{\partial \sigma_{nn}^b} & \frac{\partial F_3}{\partial \sigma_{tt}^b} & \frac{\partial F_3}{\partial \sigma_{nt}^b} & \frac{\partial F_3}{d\bar{\epsilon}_b} \\ \frac{\partial F_4}{\partial \sigma_{nn}^b} & \frac{\partial F_4}{\partial \sigma_{tt}^b} & \frac{\partial F_4}{\partial \sigma_{nt}^b} & \frac{\partial F_4}{d\bar{\epsilon}_b} \end{bmatrix} \quad (45)$$

Calculating of limiting strains is repeated for different value of  $\theta$  between 0 and 90°. It is important to note that considering of groove orientation is necessary for calculating the limit strain especially for the left hand side of FLD. Changing in the groove orientation is obtained using definition of the natural strain as follow:

$$d\epsilon = \ln \frac{l_1}{l_0} \quad (46)$$

where  $l_0$  and  $l_1$  are initial and deformed lengths, respectively. Using Equation 46 and considering Figure 5, strain increments in the rolling and transverse directions are obtained as follows:

$$d\epsilon_1 = \ln \frac{a'}{a} \Rightarrow a' = a \exp(d\epsilon_1) \quad (47)$$

$$d\epsilon_2 = \ln \frac{b'}{b} \Rightarrow b' = b \exp(d\epsilon_2) \quad (48)$$

Using Equations 47 and 48 and definition of tangent of an angle, we have:

$$\text{tg}(\theta) = \frac{a'}{b'} = \frac{a}{b} \exp(d\epsilon_1 - d\epsilon_2) = \text{tg}(\theta_0) \exp(d\epsilon_1 - d\epsilon_2) \quad (49)$$

Minimum value of major localization strain is selected among the calculation loops by variation

of  $\theta$ . The selected minimum strain for any value of  $\alpha$  is used in plotting of the FLD. This progression is shown in appendix I as a flowchart.

## 5. RESULTS AND DISCUSSIONS

In this paper, the effects of the preceding yield functions on prediction of the FLD have been studied in Al 6111-T4 and AA5XXX metals. Mechanical properties of these metals are listed in Table 1.

To calculate the limit strains, Power law relationship is selected for Al 6111-T4 and Voce hardening law is chosen for AA5XXX. Table 2 shows material constants related to these hardening laws.

Figure 6 compares the calculated FLD in AA5XXX with experimental data. To calculate the limit strains (Forming Limit Diagram) of AA5XXX  $f_0$  is selected 0.9960. As shown in Figure 6, the predicted FLD has good agreement with the experimental data. To validate the FLD of K-B yield function, the predicted FLD is compared with BBC2000 [22] and Hosford [23] yield functions. The mechanical constants related to these two yield functions for AA5XXX alloy are listed in Table 1.

In Figure 7, the predicted FLD by applying the K-B yield function is compared with the FLD of Hosford and BBC2000 yield functions. The FLD of BBC2000 and Hosford yield criteria has been also calculated by similar method in this paper. It is observed from Figure 7 that the FLD by K - B yield function is safer than the FLD by BBC2000 and Hosford yield functions with the exponent  $a = 8$ . To calculate the FLD of Al 6111-T4, the non-uniformity factor,  $f_0$ , is selected 0.9970. For this metal, the Power law is selected to describe the relation between effective strain and effective stress.  $R$  is necessary property for describing Hosford yield function in Al 6111-T4 which is 0.63. The exponent in the Hosford relationship,  $a$ , is selected 8. Figure 8 shows comparison of predicted FLD using "Karafillis-Boyce" and "Hosford" yield functions. The predicted FLD by K-B yield function has better agreement than that by Hosford yield criterion.

The calculated FLD has also been compared



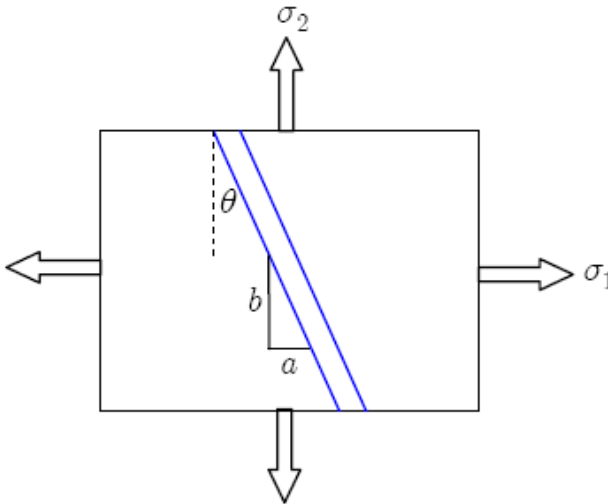


Figure 5. Groove orientation in the M - K model.

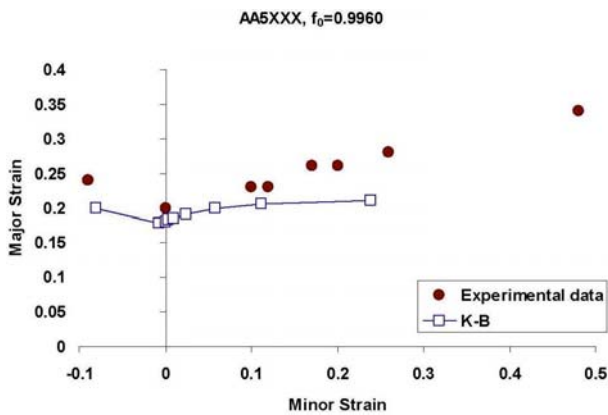


Figure 6. Comparison of Predicted FLD using K - B yield criterion and experimental data [20].

with other experimental data. Figure 9 and Figure 10 reveal the result of this comparison. As shown in all above figures, the left hand side (LHS) of FLD is linear and it is not dependent to the selection of yield function.

## 6. CONCLUSION

In this paper, to calculate the limit strains, the “Marciniak and Kuczynski” (M-K) model has been

used. The numerical method for this analysis is based on the Newton-Raphson method. Limiting strains have been calculated for Al 6111-T4 and AA5XXX alloys and compared with the experimental data. To obtain the FLD, “Karafillis and Boyce” yield function has been used. In this process, to investigate the precision of FLD by K-B yield function, its predicted FLD has been compared with the BBC2000 and Hosford yield functions in AA5XXX alloy. This study shows the FLD of K - B yield criterion is very safe and has a good agreement with the experimental results. Also, it was found that the left hand side of FLD is not dependent to the selection of yield function and

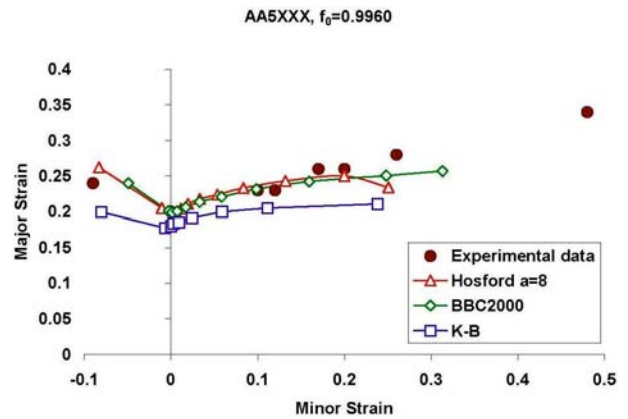


Figure 7. Comparison of FLD of different yield criteria with the experimental results [20].

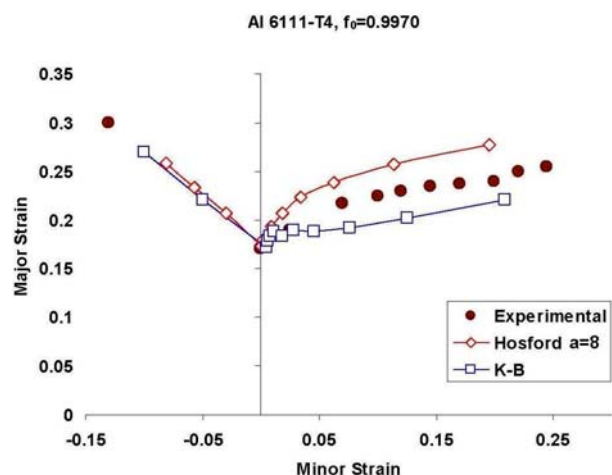


Figure 8. Comparison of Predicted FLD using K - B and Hosford yield functions and experimental data [19].

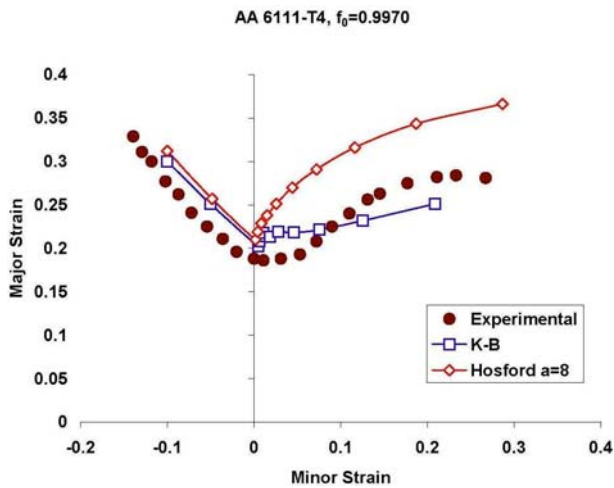


Figure 9. Comparison of FLD by K - B and Hosford yield criteria and experimental results [24].

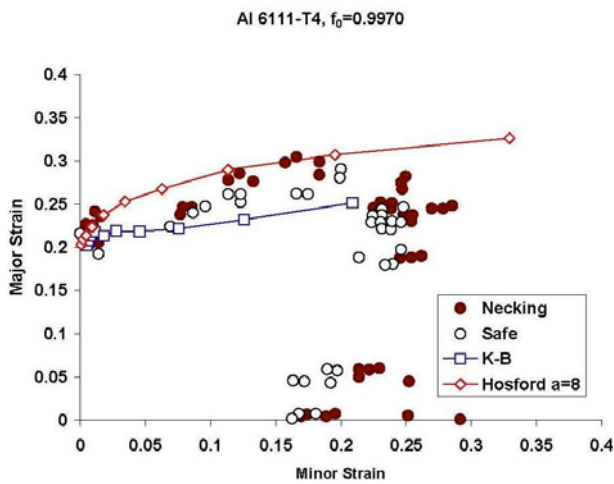


Figure 10. Comparison the right - hand side of FLD by K - B and Hosford yield criteria and experimental results [21].

has linear variation from  $FLD_0$ .

### 7. NOMENCLATURE

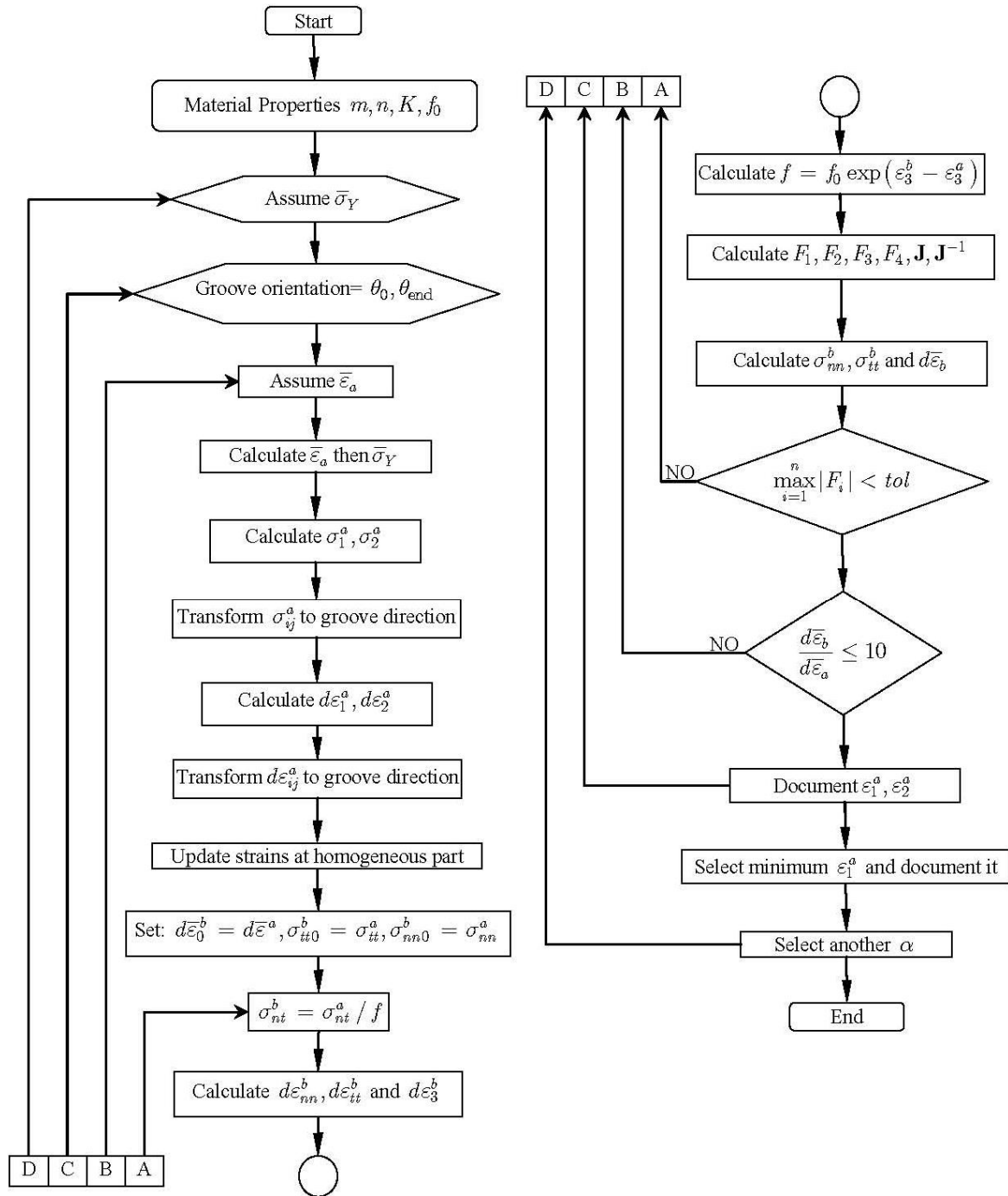
$\sigma_1, \sigma_2$	Principal stress components.
$\sigma_{nn}, \sigma_{tt}, \sigma_{nt}$	Stress components in the groove coordinate.
$\bar{\sigma}_Y$	Effective stress obtained by hardening law.

$\bar{\sigma}_Y$	Effective stress obtained by yield function.
$\varepsilon_0, K, n, m, A, B, C$	Material constants describing hardening laws.
$a, c, c_1, \dots, c_6$	Material constants describing K - B yield function.
$\bar{a}, \bar{b}, \bar{c}, M, N, P, Q, R$	Material constants describing BBC2000 yield function.
$R$	Normal anisotropy.
$\bar{\varepsilon}$	Effective plastic strain.
$\dot{\bar{\varepsilon}}$	Rate of effective plastic strain.
$d\bar{\varepsilon}$	Effective plastic strain increment.
$d\varepsilon_{nn}, d\varepsilon_{tt}, d\varepsilon_{nt}$	Strain increments in the groove coordinate.
$d\varepsilon_1, d\varepsilon_2, d\varepsilon_3$	Strain increments in the material coordinate.
$a$	Ratio of stresses along the strain path.
$T$	Rotation matrix.
$d\lambda$	Plastic multiplier.
$F_{nm}, F_{nt}$	Force equations in the groove directions.
$f$	Non-uniformity factor.
$\delta x$	Newton's step.
$J$	Jacobian matrix.
$\theta$	Angle between the groove coordinates and the material coordinates.
$\lambda$	Newton step length.

### 8. REFERENCES

- Keeler, S. P. and Backofen, W. A., "Plastic Instability and Fracture in Sheets Stretched Over Rigid Punches", *Transactions of The ASM*, 56, (1963), 25-48.
- Goodwin, G. M., "Application of Strain Analysis to Sheet Metal Forming Problems in the Press Shop", Society of Automotive Engineers, Technical Paper No., (1968), 680093.
- Keeler, S. P., "Determination of Forming Limits in Automotive Stampings", Society of Automotive Engineers, Technical paper No., (1965), 650535.
- Marciniak, M. and Kuczynski, K., "Limit Strains in the Processes of Stretch - Forming Sheet Metals", *Int. J. Mech. Sci.*, 9, (1967), 609-20.
- Marciniak, Z., Kuczynski, K. and Pokora, T., "Influence of the Plastic Properties of a Material on the Sheet Forming Limit Diagram for Sheet Metal in Tension",

APPENDIX I. The Progression Flowchart for Prediction of FLD.



*Int. J. Mech. Sci.*, (1973), 15: 789-805.

6. Van Minh, H., Sowerby, R. and Duncan, J. L., "Probabilistic Model of Limit Strains in Sheet Metal",

*Int. J. Mech. Sci.*, 17, (1975), pp. 339-349.

7. Yamaguchi, K. and Mellor, P. B., "Thickness and Grain Size Dependence of Limit Strains in Sheet Metal

- Stretching”, *Int. J. Mech. Sci.*, 18, (1976), 85-93.
8. Tadros, A. K. and Mellor, P. B., “Some Comments on the Limit Strains in Sheet Metal Stretching”, *Int. J. Mech. Sci.*, 17, (1975), pp. 203-208.
  9. Barata da Rocha, F. B. and Jalinier, J. M., “Prediction of the Forming Limit Diagrams of Anisotropic Sheets in Linear and Non - Linear Loading”, *Mater. Sci. Eng.*, 68, (1984–1985), 151–64.
  10. Kuroda, Mand. and Tvergaard, V., “Forming Limit Diagrams for Anisotropic Metal Sheets with Different Yield Criteria”, *Int. J. Solids Struct.*, 37, (2000), 5037–59.
  11. Cao, J., Yao, H., Karafillis, A. and Boyce, Mary C., “Prediction of Localized Thinning in Sheet Metal Using a General Anisotropic Yield Criterion”, *Int. J. of Plasticity*, 16, (2000), 1105-1129.
  12. Kuroda, Mits. and Tvergaard, V., “Forming Limit Diagrams for Anisotropic Metal Sheets with Different yield criteria”, *Int. J. of Solids and Struct.*, 37, (2000), 5037-5059.
  13. Butuc, M. C., Barata da Rocha, A., Gracio, J. J. and Ferreira Duarte, J., “A more general model for forming limit diagrams prediction” *J. Mater. Process. Technol.*, (2002), 125–126, 213–18.
  14. Banabic, D., Aretz, H., Paraianu, L. and Jurco, P., “Application of Various FLD Modeling Approaches”, *Modeling Simul. Mater. Sci. Eng.*, 13, (2005), 759–769.
  15. Voce, E., “The Relationship Between Stress and Strain for Homogeneous Deformation”, *J. Inst. Met.*, 74, (1948), 537–540.
  16. Armijo, L., “Minimization of Functions Having Lipschitz Continuous First Partial Derivatives”, *Pacific J. Math.*, (1966), 6:1-3.
  17. Karafillis, A. P. and Boyce, M. C., “A General Anisotropic Yield Criterion Using Bounds and Transformation Weighting Tensor”, *J. Mech. Phys. Solids*, 41, (1993), 1859.
  18. Yao, H. and Cao, J., “Prediction of Forming Limit Curves Using an Anisotropic Yield Function with Prestrain Induced Back Stress”, *Int. J. Plasticity*, 18, (2002), 1013-1038.
  19. Chow, C. L. and Yang, X – J., “Prediction of the Forming Limit Diagram on the Basis of the Damage Criterion under Non - Proportional Loading”, *Proceed. Instit. Mech. Eng., 4: ProQuest Science Journals*, (2001), 215.
  20. Butuc, M. C., Banabic, D., Barata da Rocha, A., Gracio, J. J., Ferreira Duarte, J., Jurco, P. and Comsa, D. S., “The Performance of Yld96 and BBC2000 Yield Functions in Forming Limit Prediction”, *J. of Mater. Process. Tech.*, (2002), 125-126, 281-286.
  21. Siguang, Xu, and Weinmann, Klaus J., “Prediction of Forming Limit Curves of Sheet Metals Using Hill’s 1993 User - Friendly Yield Criterion of Anisotropic Materials”, *Int. J. Mech. Sci.*, (1998), 40, 913-925.
  22. Barlat, F. and Lian, J., “Plastic Behavior and Stretchability of Sheet Metals. Part I: A Yield Function for Orthotropic Sheet Under Plane Stress Conditions”, *Int. J. Plasticity*, (1989), 5, 51-56.
  23. Hosford, W. F., “On Yield Loci of Anisotropic Cubic Metals”, *7th North American Metalworking Research Conference Proceedings*, SME Dearborn, Michigan, (1979), 191.
  24. Wu, P. D., Graf, A., MacEwen, S. R., Lloyd, D. J., Jain, M. and Neale, K. W., “On Forming Limit Stress Diagram Analysis”, *Int. J. Solids and Struct.*, (2005), 42, 2225-2241.